010598   001N

Feedback Control of Linear Turbulence Using Electromagnetic Microtiles

Sahjendra N. Singh
University of Nevada at Las Vegas

Promode R. Bandyopadhyay
Weapons Technology and Undersea Systems Department

UNCLASSIFIED

Naval Undersea Warfare Center Division
Newport, Rhode Island

PREFACE

Reviewed and Approved: 23 August 1996

J. C. S. Meng
Head, Weapons Technology and
Undersea Systems Department

REPORT DOCUMENTATION PAGE

Public reporting for this collection of information is estimated to average 1 hour per response, including the time for reviewing instructions, searching existing data sources, gathering and maintaining the data needed, and completing and reviewing the collection of information. Send comments regarding this burden estimate or any other aspect of this collection of information, including suggestions for reducing this burden, to Washington Headquarters Services, Directorate for Information Operations and Reports, 1215 Jefferson Davis Highway, Suite 1204, Arlington, VA 22202-4302, and to the Office of Management and Budget, Paperwork Reduction Project (0704-0188), Washington, DC 20503.

1. AGENCY USE ONLY *(Leave blank)*	2. REPORT DATE 23 August 1996	3. REPORT TYPE AND DATES COVERED Final

4. TITLE AND SUBTITLE

Feedback Control of Linear Turbulence Using Electromagnetic Microtiles

5. FUNDING NUMBERS

6. AUTHOR(S)

S.N. Singh (University of Nevada at Las Vegas)
P.R. Bandyopadhyay

7. PERFORMING ORGANIZATION NAME(S) AND ADDRESS(ES)

Naval Undersea Warfare Center Division
1176 Howell Street
Newport, RI 02841-1708

8. PERFORMING ORGANIZATION REPORT NUMBER

TR 10,598

9. SPONSORING/MONITORING AGENCY NAME(S) AND ADDRESS(ES)

Office of Naval Research
800 North Quincy Street
Arlington, VA 22217-5660

10. SPONSORING/MONITORING AGENCY REPORT NUMBER

11. SUPPLEMENTARY NOTES

12a. DISTRIBUTION/AVAILABILITY STATEMENT

Approved for public release; distribution is unlimited.

12b. DISTRIBUTION CODE

13. ABSTRACT *(Maximum 200 words)*

A small, axisymmetric body with numerous millimeter-scale microtiles embedded with thin arrays of magnets and electrodes has been designed and built at the Naval Undersea Warfare Center Division, Newport, RI. For sea water turbulence control at high Reynolds numbers, these microtiles produce Lorentz forces of preferred orientation by crossing electric and magnetic fields. This report presents a system-theory approach to control of a two-dimensional flow on a flat plate using Lorentz forces produced by these microtiles. Beginning with the two-dimensional Navier-Stokes equations of motion, a finite, dimensional, linear state variable, approximate model is obtained using Galerkin's procedure. Based on this model, linear feedback control laws are obtained to achieve stabilization of the perturbed flow to the base flow. It is shown that spatially distributed longitudinal or surface-normal forces stabilize the flow perturbations. However, for lower wave numbers, longitudinal forces are more effective because surface-normal forces require larger electrode voltages for the same response characteristics. Simulation results are presented to show how stabilization is accomplished in the closed-loop system.

14. SUBJECT TERMS

Shear Flow	Turbulence Control	Microtiles	Turbulent Boundary Layers
Electromagnetics	Lorentz Forces	Drag Reduction	Reynolds Numbers

15. NUMBER OF PAGES
26

16. PRICE CODE

17. SECURITY CLASSIFICATION OF REPORT Unclassified	18. SECURITY CLASSIFICATION OF THIS PAGE Unclassified	19. SECURITY CLASSIFICATION OF ABSTRACT Unclassified	20. LIMITATION OF ABSTRACT SAR

TABLE OF CONTENTS

LIST OF ILLUSTRATIONS

FEEDBACK CONTROL OF LINEAR TURBULENCE USING ELECTROMAGNETIC MICROTILES

1. INTRODUCTION

Control of turbulence leads to reduction in the viscous drag and suppression of turbulence-induced noise. Via direct numerical simulation of a low Reynolds number channel flow over a riblet surface, Crawford and Karniadakis[1] have shown that drag reduction is uniquely related to the suppression of the surface-normal component of turbulence near the wall. Bushnell,[2] Bandyopadhyay,[3] and Gad-el-Hak[4] describe research done in this area. Several experimental and computational studies have also focused on the delay of boundary-layer transition through wave suppression by introducing waves of appropriate amplitudes and phases.[5,6,7] In recent studies, Joshi[8] and Joshi et al.[9] have taken system-theory approaches to the channel flow control by suction and injection at the wall. In a system-theory approach, the model is initially represented by a set of first-order differential equations, and then modern system and control theory is applied to the model design and to system analyses.

A Lorentz force field is produced when electric and magnetic fields are applied in an electrically conducting medium. The potential application of Lorentz forces for drag reduction and turbulence control has been investigated by Henoch and Stace[10] and Nosenchuck and Brown.[11] These approaches to electromagnetic turbulence control, however, do not use feedback algorithms. Nosenchuck and Brown[11] have pulsed a surface-normal Lorentz force in an attempt to minimize the outward component of the surface-normal perturbations. On the other hand, Meng[12] has proposed a sensor-based active feedback control scheme and has modeled the turbulence production process as the appearance of a sequence of organized motions given by the probabilistic distributions of their scales. Meng then proposed a Markov chain control scheme that uses sensors and attempts to control the Lorentz forces over all phases of the turbulence regeneration process. At the Naval Undersea Warfare Center (NUWC) Division, Newport, RI, Bandyopadhyay has designed two-dimensional thin arrays of electromagnetic tiles with spatial scales on the order of millimeters that are suitable for high Reynolds number turbulence control.[13] The electromagnetic forces produced by these microtiles are confined to within 1 millimeter from the wall and are promising for the boundary-layer turbulence control at high Reynolds numbers.[14]

Low Reynolds number laminar flow experiments have indicated that the NUWC microtiles produce "pillows" of vorticity that scale with their size. It is believed that the microtiles redistribute the prevailing vorticity in the shear flow but do not introduce vorticity into the flow. The observations of the pillows of vorticity have been later confirmed by direct numerical simulation.[15] The microtiles can be described as hairpin vortex-generators. Further numerical simulations of a turbulent channel flow over an array of two microtiles at low Reynolds numbers and subjected to a steady power supply indicate that an 8-percent suppression of turbulence can be achieved by the low-power microtiles.[16] In this simulation, the channel flow Reynolds number *Re* was 50,470.8, based on channel half-width and maximum centerline velocity. The magnets and electrodes in each microtile were arranged in a checkerboard pattern, where one *ideal* Lorentz force was vertical (in reality, one force is three-dimensional near one corner). Within a microtile, the open area between the magnets and electrodes measured 4 mm x 1 mm in the streamwise and

cross-stream directions, respectively. The applied maximum magnetic field strength B_0 was 0.6 T and the voltage E was 6.0 V. An array of 2-x-2 microtiles was considered, and the turbulence suppression reported above was attained at 12 wall units from 1 surface.

The present study focuses on the control of a two-dimensional turbulent boundary layer on a flat plate and explores the feasibility of a closed-loop control. The system-theory approach taken here is similar to that of Joshi,[8,9] however the Lorentz force field produced by microtiles is the control mechanism. Moreover, a flat-plate, boundary-layer flow is, because of the nature of boundary conditions, relatively complicated compared with the channel flow. Although turbulence control for any finite perturbation is the final goal, this study is limited to control of small perturbations in the base flow. The present approach to control via Navier-Stokes equations is rooted in the structural modeling of a turbulent boundary layer as advanced by Perry and Chong[17] and by Bandyopadhyay and Balasubramanian.[18, 19] Structural modeling of a turbulent boundary layer is better suited for feedback control than is statistical turbulence modeling. In conventional turbulence modeling, a turbulent flow is described by the Reynolds decomposition, where it is said to be composed of a time-mean flow and random perturbations. The time-mean flow is described statistically via closure models. However, in this report, along the lines of Bandyopadhyay and Balasubramanian,[18, 19] a turbulent boundary layer is described to be composed of a laminar-like base flow and random perturbations. Because feedback control requires deterministic signals, the perturbations are described via Fourier series and not statistically. To date there has been no study on feedback electromagnetic turbulence or any control that could probably achieve a higher level of turbulence suppression than an open-loop control can achieve.

The problem of turbulence control is complex because the governing equations of motion are nonlinear and infinitely dimensional and control theory for infinite-dimensional systems is not well developed. In this report, a finite-dimensional approximate model is derived based on the Galerkin procedure and Chebyshev polynomials.[8,9,20,21,22] Based on this model, linear feedback control laws are derived using optimal control techniques and also by using a simple feedback of wall-shear stress for the stabilization of the perturbed flow to the base flow. It is shown that the unstable modes can be controlled by longitudinal as well as surface-normal forces. However, for lower wave numbers, longitudinal forces are more effective and require smaller electrode voltages for control compared with surface-normal forces. It is shown that a judicious choice of spatial distribution of Lorentz forces is important for designing stabilizing controllers, and this requires proper activation of the electrodes. Numerical results are obtained to show that, in the closed-loop system, asymptotic stabilization of the flow is accomplished using moderate input voltage for small perturbations.

This report is organized as follows. Section 2 presents the mathematical model and addresses the control problem. A linear, finite-dimensional model is obtained in section 3. Section 4 presents control laws, and simulation results are given in section 5.

2. MATHEMATICAL MODEL AND CONTROL PROBLEM

A two-dimensional flow on a flat plate of length ℓ is considered. The x-axis is in the flow direction, and the y-axis is normal to the plate. The free stream velocity is U_∞. Reference values $h = (\delta_m/2)$, U_∞, and (h/U_∞) are chosen for the normalization of length, velocity, and time, where δ_m is the boundary-layer thickness (location where 99.5 percent of the freestream speed is reached). Suppose that r independent voltages are applied to the microtiles for control. It has been found that Lorentz forces are proportional to the voltages applied to the electrodes because permanent magnets are used.

The nondimensionalized Navier-Stokes equations of motion for the two-dimensional flow are given by

$$\left(\partial u/\partial t\right)+u\left(\partial u/\partial x\right)+v\left(\partial u/\partial y\right)=-\left(\partial p/\partial x\right)+Re^{-1}\nabla^2 u+k_0 F_1(x,y,E)$$
$$\left(\partial v/\partial t\right)+u\left(\partial v/\partial x\right)+v\left(\partial v/\partial y\right)=-\left(\partial p/\partial y\right)+Re^{-1}\nabla^2 v+k_0 F_2(x,y,E), \tag{1}$$

and the continuity equation is

$$\left(\partial u/\partial x\right)+\left(\partial v/\partial y\right)=0,$$

where $k_0 = h/\left(\rho U_\infty^2\right)$; u and v are the longitudinal and lateral velocities; p is the pressure field, ρ is the density of the fluid; Re is the Reynolds number, 50,470.8; F_1 and F_2 are the longitudinal and lateral Lorentz forces; and $E \in R^r$ is the vector of applied voltages to electrodes. At the wall, y is -1, and
$y = 1$ at the outer edge of the boundary layer at $x = \ell_1 = \ell/h$.

For the basic flow, approximate solutions of the boundary layer are given as

$u = U(y) = U_\infty g(\eta),$
$\eta = (y + 1)h/\delta(x),$

where $g(\eta)$ is assumed to be one of the following forms:[23]

$$g(\eta) = \sin\left(\pi \eta/2\right)$$
or
$$g(\eta) = 2\eta - 2\eta^3 + \eta^4.$$

Although the boundary layer on a flat plate is a function of x and y, to simplify model derivation, a base flow of the form

$$u = U(y), v = 0, p = P(x)$$

is assumed. This is obtained by replacing $\delta(x)$ with δ_m, a constant in the definition of η. For the perturbed motion,

$$u = U(y) + u_1(x,y,t), v = v_1(x,y,t), p = P + p(x,y,t), \tag{2}$$

where u_1, v_1, and p represent small perturbations in the base flow. It will be seen later that, when the base flow is chosen to also be a function of x for linearization, a model is obtained in which all the modes are coupled—creating complexity in controller design. Restricting the region from the leading edge of the plate causes the base flow to be weakly dependent on x.[23]

By substituting the values in equation (2) in equation (1), neglecting higher order terms, eliminating p_1 (by subtracting partial derivative of the second equation with respect to x from the partial derivative of the first equation with respect to y in equation (1)), and using the continuity equation, the linear dynamics are obtained by

$$\left(\partial^2 u_1/\partial t\partial y\right) - \left(\partial^2 v_1/\partial t\partial x\right) + U(y)\left(\left(\partial^2 u_1/\partial x\partial y\right) - \left(\partial^2 v_1/\partial x^2\right)\right) + U^{(2)}v_1$$
$$= Re^{-1}\left(\left(\partial^3 u_1/\partial x^2\partial y\right) + \left(\partial^3 u_1/\partial y^3\right) - \left(\partial^3 v_1/\partial x\partial y^2\right) - \left(\partial^3 v_1/\partial x^3\right)\right)$$
$$+ k_0\left(\left(\partial F_1/\partial y\right) - \left(\partial F_2/\partial x\right)\right), \tag{3}$$

where $U^{(2)} = d^2 U(y)/dy^2$, and the arguments of various functions are suppressed for simplicity. The continuity equation for the perturbations is

$$\left(\partial u_1/\partial x\right) + \left(\partial v_1/\partial y\right) = 0. \tag{4}$$

Theoretically, the boundary conditions are such that u_1 and v_1 tend toward zero as y tends toward infinity. However, the effect of viscosity is negligible beyond the outer edge of the boundary layer. Therefore, in order to obtain a simplified model, the boundary conditions are assumed to be

$$u_1(-1) = v_1(-1) = 0,$$
$$u_1(1) = v_1(1) = 0. \tag{5}$$

The problem is to design a feedback control system so that, in the closed-loop system, perturbations $u_1(x, y, 0)$ and $v_1(x, y, 0)$ at $t = 0$ asymptotically converge to zero as t tends toward infinity. In this case, small but arbitrary perturbations in velocities u and v decay to zero, and the perturbed flow tends toward the base flow asymptotically.

4

3. A FINITE DIMENSIONAL MODEL

In this section, a finite dimensional model is obtained using the Galerkin's method with the Chebyshev polynomials as basis.[8, 20-22] The choice of these Chebyshev polynomials has given useful results in the channel flow control problem of Joshi.[8, 9] Some other independent set of functions can be used for derivation. However, the convergence property of the derived model to the actual system depends on the choice of basis.

To this end, a perturbed stream function $\psi_1(x, y, t)$ is chosen for the system (equation (3)) such that

$$u_1 = \partial \psi_1(x, y, t)/\partial y,$$
$$v_1 = -\partial \psi_1(x, y, t)/\partial x \tag{6}$$

satisfy equation (4). Substituting the values in equation (6) in equation (3) provides a single, partial differential equation given by

$$\left(\partial^3 \psi_1/\partial t \partial x^2\right) + \left(\partial^3 \psi_1/\partial t \partial y^2\right) + U(y)\left(\left(\partial^3 \psi_1/\partial x \partial y^2\right) + \left(\partial^3 \psi_1/\partial x^3\right)\right)$$
$$-U^{(2)}\left(\partial \psi_1/\partial x\right) = \mathrm{Re}^{-1}\nabla^2\left(\nabla^2 \psi_1\right) + k_0\left(\left(\partial F_1/\partial y\right) - \left(\partial F_2/\partial x\right)\right), \tag{7}$$

where

$$\nabla^2 = \left(\partial^2/\partial x^2\right)\left(\partial^2/\partial y^2\right).$$

Motivated by the choice of periodic function of x in the derivation of the Orr-Somerfield equation[22] and due to the periodic fluctuations of the velocities in the longitudinal direction, a hypothesis can be formulated for a series solution for the stream function of the form

$$\psi_1(x, y, t) = \sum_{n=0}^{\infty}\sum_{m=0}^{\infty}\left(a_{nm}(t)\cos(n\alpha_0 x) + b_{nm}(t)\sin(n\alpha_0 x)\right)L_m(y), \tag{8}$$

where $L_m(y)$, $(m = 0, 1, \ldots, \infty)$ are the set of basis functions formed by a suitable combination of Chebyshev polynomials that satisfy the boundary conditions (equation (5)). In view of equations (5), (6), and (8), it easily follows that functions $L_m(y)$ must satisfy

$$L_m(-1) = L_m(1) = 0,$$
$$\partial L_m(-1)/\partial y = \partial L_m(1)/\partial y = 0. \tag{9}$$

Here the fundamental wave number is $\alpha_0 = (2\pi/\ell_1)$; $n\alpha_0$ is the wave number of the nth harmonic term in the series solution, $b_{0m} = 0$; and a_{nm} and b_{nm} are the time-dependent, generalized coordinates (amplitudes of modes).

Substituting equation (8) in equation (7) and truncating the series to obtain a finite dimensional model gives

$$\sum_{n=0}^{N}\sum_{m=0}^{M}\left(\dot{a}_{nm}\cos(n\alpha_0 x)+\dot{b}_{nm}\sin(n\alpha_0 x)\right)\left(L_m^{(2)}(y)-(n\alpha_0 x)^2 L_m(y)\right)$$

$$=\sum_{n=0}^{N}\sum_{m=0}^{M}\left(-a_{nm}\sin(n\alpha_0 x)+b_{nm}\cos(n\alpha_0 x)\right)n\alpha_0\left(\left((n\alpha_0)^2 U+U^{(2)}\right)L_m(y)-UL_m^{(2)}(y)\right)$$

$$+Re^{-1}\left(a_{nm}\cos(n\alpha_0 x)+b_{nm}\sin(n\alpha_0 x)\right)$$

$$\left((n\alpha_0)^4 L_m(y)+L_m^{(4)}-2(n\alpha_0 x)^2 L_m^{(2)}(y)\right)+k_0\left(\partial F_1/\partial y-\partial F_2/\partial x\right), \qquad (10)$$

where an overdot denotes differentiation with respect to time, and $L_m^{(i)}(y)=d^i L_m(y)/dy^i$. In this derivation, it is assumed that $(M+1)$ basis functions $L_m(y)$ and N sinusoidal functions give a reasonable approximate model. If the design with chosen values for M and N is unsatisfactory and the residual modes in the closed-loop system are not small, then the controller needs to be redesigned using a model with larger values for M and N.

It has been shown in reference 13 that for each volt applied to the electrodes, the Lorentz force can be accurately expressed as $k_1\exp(-q_0 d)$, where d is the lateral distance from the wall and it is negligible for $d>2$ mm. To this end, spatially distributed Lorentz forces are expressed in a Fourier series of the form $(i=1, 2)$

$$F_i=k\sum_{n=0}^{N}\left(F_{ni1}\cos(n\alpha_0 x)+F_{ni2}\sin(n\alpha_0 x)\right)\exp(qy)E, \qquad (11)$$

where $y\in[-1, y_m]$, $k=k_0 k_1\exp(q)$, $q=-q_0 h$, and F_{nik} is an r-row vector. It is assumed that the Lorentz force is negligible for $y\geq y_m$. The values of q_0 and k_1 are obtained from the Lorentz force plot given in reference 13.

Because the trigonometric functions form an orthogonal set, substituting equation (11) in equation (10), multiplying equation (10) by $\cos(n\alpha_0 x)$ $(\sin(n\alpha_0 x))$, and integrating over $[0,\ell_1]$ give the differential equations for a_{nm} (b_{nm}) given by

$$\sum_{m=0}^{M}\left(\dot{a}_{nm}\left(L_m^{(2)}(y)-(n\alpha_0)^2 L_m(y)\right)\right)=\sum_{m=0}^{M}b_{nm}n\alpha_0\left(\left((n\alpha_0)^2 U+U^{(2)}\right)L_m(y)-UL_m^{(2)}(y)\right)$$

$$+Re^{-1}a_{nm}\left((n\alpha_0)^4 L_m(y)+L_m^{(4)}(y)-2(n\alpha_0)^2 L_m^{(2)}(y)\right)$$

$$+k(qF_{n11}-n\alpha_0 F_{n22})\exp(qy)E,$$

$$\sum_{m=0}^{M}\left(\dot{b}_{nm}\left(L_m^{(2)}(y)-(n\alpha_0)^2 L_m(y)\right)\right)=\sum_{m=0}^{M}-a_{nm}n\alpha_0\left(\left((n\alpha_0)^2 U+U^{(2)}\right)L_m(y)-UL_m^{(2)}(y)\right)$$

$$+Re^{-1}b_{nm}\left((n\alpha_0)^4 L_m(y)+L_m^{(4)}(y)-2(n\alpha_0)^2 L_m^{(2)}(y)\right)$$

$$+k(qF_{n12}+n\alpha_0 F_{n21})\exp(qy)E. \qquad (12)$$

The inner product of $L_s(y)$ and $L_m(y)$ is defined as[22]

$$L_{sm}=\left(L_s(y), L_m(y)\right)=\int_{-1}^{+1}L_s(y)L_m(y)\left(1-y^2\right)^{-0.5}dy. \qquad (13)$$

6

Define matrices as $(s = 0,1,\ldots,M; m = 0,1,\ldots,M)$

$$D_{n0} = \left(\left(D_{n0}\right)_{sm}\right) = \left(L_s, \left(L_m^{(2)} - \left(n\alpha_0\right)^2 L_m\right)\right),$$

$$D_{n1} = \left(\left(D_{n1}\right)_{sm}\right) = \left(L_s, \left(\left(n\alpha_0\right)^4 L_m + L_m^{(4)} - 2\left(n_0\alpha_0\right)^2 L_m^{(2)}\right)\right),$$

$$D_{n2} = \left(\left(D_{n2}\right)_{sm}\right) = \left(L_s, \left(-UL_m^{(2)} + \left(\left(n\alpha_0\right)^2 U + U^2\right)L_m\right)\right),$$

$$L_y = \left(\left(L_0, \exp(qy)\right),\ldots,\left(L_m, \exp(qy)\right)\right)^T,$$

$$B_{n1} = kL_y\left(qF_{n11} - n\alpha_0 F_{n22}\right),$$

$$B_{n2} = kL_y\left(qF_{n12} + n\alpha_0 F_{n21}\right), \tag{14}$$

where $(D_{ni})_{sm}$ denotes the s—mth element of matrix D_{ni}, T denotes transposition, and in the computation of L_y integration is performed only over $[-1, y_m]$ where the Lorentz forces are significant.

By using the definitions of matrices in equation (14), equation (12) is written in a matrix notation as

$$D_{n0}\dot{a}_n = D_{n1}a_n + D_{n2}b_n + B_{n1}E,$$

$$D_{n0}\dot{b}_n = D_{n2}a_n + D_{n1}b_n + B_{n2}E, \tag{15}$$

where $a_n = (a_{n0},\ldots,a_{nM})^T$ and $b_n = (b_{n0},\ldots,b_{nM})^T$. The state subvector $x_n = (a_n^T, b_n^T)^T$ is associated with the wave number $n\alpha_0$ and it is described by

$$\dot{x}_n = A_n x_n + B_n E, \quad \text{for } n \neq 0, \tag{16}$$

where

$$A_n = \begin{pmatrix} D_{n0}^{-1}D_{n1} & D_{n0}^{-1}D_{n2} \\ -D_{n0}^{-1}D_{n2} & D_{n0}^{-1}D_{n1} \end{pmatrix},$$

$$B_n = \left(\left(D_{n0}^{-1}B_{n1}\right)^T, \left(D_{n0}^{-1}B_{n2}\right)^T\right)^T.$$

For $n = 0$,

$$\dot{x}_0 = A_o x_0 + B_0 E, \tag{17}$$

where $x_0 = a_0 = (a_{00},\ldots,a_{0M})^T$, $A_0 = D_{00}^{-1}D_{01}$, and $B_0 = D_{00}^{-1}B_{01}$. The vector

$$x_a = \left(x_0^T,\ldots,x_N^T\right) = \left(a_0^T; a_1^T, b_1^T;\ldots; a_N^T, b_N^T\right)^T$$

is called the state vector of the system (equations (16) and (17)), because x_a completely describes the perturbed velocity vector in the boundary layer. For a given initial condition $x_a(0)$ and the electrode voltage $E(t)$, equations (16) and (17) can be solved for:

$$x_i(t), i = 0, 1, \ldots, N, \quad t \geq 0.$$

These time-dependent coefficients are substituted in equation (8) to obtain the perturbed stream function and the velocity vector field.

It is interesting to note that in view of equation (16), the dynamics associated with various wave numbers are decoupled for $E = 0$. The decoupling of modes is not possible if x-dependent base flow is taken. It will be seen that decoupling considerably simplifies control system design.

Now the problem of flow control is solved by deriving feedback control laws of the form

$$E = -Kx_c,$$

such that, in the closed-loop system, $x_a(t)$ asymptotically tends toward zero, where x_c is a chosen subvector of the state vector x_a.

4. CONTROL SYSTEMS

Using equations (16) and (17), the complete system can be written in a state variable form:

$$\dot{x}_a = A_a x_a + B_a E, \tag{18}$$

where $A_a = \text{diag}(A_0, A_1, \ldots, A_N)$ and the input influence matrix is $B_a = \left(B_0^T, B_1^T, \ldots, B_N^T\right)^T$. To determine the fluctuations of the wall-shear stress at a point x^*, because it is proportional to du_1/dy, consider an output variable $y_a = du_1/dy(x^*, y = -1, t)$ written as

$$y_a = C_a x_a, \tag{19}$$

where the output matrix C_a is

$$C_a = \left(c_{a0}, \ldots, c_{aN}\right),$$
$$L_c = \left(L_0^{(2)}(-1), \ldots, L_M^{(2)}(-1)\right),$$
$$c_{a0} = L_c,$$

and for $n \neq 0$,

$$c_{an} = \left(\cos\left(n\alpha_0 x^*\right)L_c, \sin\left(n\alpha_0 x^*\right)L_c\right).$$

This output can be used for feedback for stabilization or to directly control y_a.

The concept of controllability plays an important role in system theory.[24] The system (equation (18)) is said to be controllable if, given any two arbitrary points x_a^1 and x_a^2 in the state space, there exists a control E that can steer the system (equation (18)) from x_a^1 to x_a^2 in a finite time. The system is controllable if, and only if, the controllability matrix CO defined as

$$CO = \left(B_a, A_a B_a, \ldots, A_a^{s-1} B_a\right),$$

has rank $s = (2N+1)(M+1)$, which is the dimension of state vector x_a. The spatial distribution of the Lorentz forces must be chosen to satisfy the controllability conditions. For the controllable system, a linear feedback law to stabilize the system can be chosen.

For clarity, it is assumed that the electrode voltage $E(t)$ is a scalar function. The design for the multi-input system can be similarly done. It is interesting to note that in the model (equation (18)), not all modes are unstable. For the chosen parameters identified in section 5, it is found that only matrix A_1 associated with the fundamental wave number α_0 is unstable, the remaining matrices A_i are stable. Because the electrode voltage is limited, it is a good idea to design a control system to stabilize only the dynamics of unstable wave numbers and to leave the responses of other modes unaltered. The dynamics of the unforced system are decoupled, therefore, one way to preserve the dynamics of the stable modes is to choose the spatial distribution of the Lorentz forces such that the control influence matrix B_k of the stable modes are null; that is,

$$B_0 = 0, \ B_n = 0, \ n \neq 1. \tag{20}$$

For this choice, when the feedback loop is closed to stabilize the unstable mode using the measured signal y_a, control input will not excite the remaining modes.

The condition in equation (20) can be satisfied by choosing F_1 and F_2 of the form ($i = 1, 2$)

$$F_i = k_1[F_{1i1} \cos \alpha_0 x + F_{1i2} \sin \alpha_0 x] \exp(qy) E , \tag{21}$$

where $\left(F_{1i1}^2 + F_{1i2}^2 \right)^{1/2} = 1$. The sinusoidal distribution of Lorentz forces requires appropriate activation of the electrodes. If other harmonic terms are present in equation (21), the dynamics of other wave numbers will be excited when the measured signal y_a is fed back.

Because either the longitudinal or the surface-normal force for control can be chosen, a question arises concerning the effectiveness of Lorentz forces for control. In view of the input influence matrices B_{n1} and B_{n2} in equation (14), if

$$n\alpha_0 > -q ,$$

the input influence matrix B_n is larger when surface-normal force is used. However, for smaller wave numbers not satisfying the above inequality, the longitudinal force is preferable for stabilization because smaller electrode voltage will be needed for control. In section 5.2 a simple feedback law using wall-shear stress (or $du_1/dy(x^*, y = -1, t)$ for stabilization is simulated.

Several control techniques for linear systems are available for the control system design and can be applied to obtain different response characteristics and to meet design specifications. For the choice of Lorentz force as given in equation (21), the optimal control technique can be used. Consider the dynamics associated with the fundamental wave number

$$\dot{x}_1 = A_1 x_1 + B_1 E , \tag{22}$$

which is unstable. Here $x_1 = \left(a_1^T, b_1^T \right)^T$ is the state vector associated with the wave number α_0. The optimal control is obtained by minimizing a quadratic performance index of the form

$$J = \int_0^\infty \left(x_1^T Q x_1 + \lambda E^2 \right) dt , \tag{23}$$

where Q is a positive definite symmetric matrix, and $\lambda > 0$. The matrices Q and λ are selected to weigh the relative importance of performance measures caused by the state vector perturbations x_1 and the electrode voltage $E(t)$. The optimal control law is

$$E = -\lambda^{-1} B_1^T R x_1 = -K x_1, \tag{24}$$

where the positive definite symmetric matrix R is the solution of the Riccati equation[24]

$$RA_1 + A_1^T R - RB_1 \lambda^{-1} B_1^T R + Q = 0,$$

and K is a row vector of dimension $2(M+1)$.

Substituting linear control law (equation (24)) in equation (22) gives the closed-loop system:

$$\dot{x}_1 = \left(A_1 - B_1 K\right)x_1,$$

for which the matrix $\left(A_1 - B_1 K\right)$ is Hurwitz (i.e., all the eigenvalues of $\left(A_1 - B_1 K\right)$ have negative real parts). Thus, in the closed-loop system, $x_1(t)$ asymptotically tends toward zero, which implies that the perturbations u_1 and v_1 decay to zero as well. The response characteristics for the state vector x_1 depend on the eigenvalues of the matrix $\left(A_1 - B_1 K\right)$.

Substituting $Qy_1^2, Q > 0$ in place of $x_1^T Q x_1$ in the performance index can be done for minimization, where

$$y_1 = \left(\cos\left(\alpha_0 X^*\right)L_c, \sin\left(\alpha_0 x^*\right)L_c\right)x_1 \underline{\underline{\Delta}} c_1 x_1 \tag{25}$$

for directly influencing du_1/dy at $x = x^*$. By a proper selection of the weighting matrix, Q, and the scalar, λ, a tradeoff between the speed of convergence of the perturbed state to the equilibrium state and the magnitude of the electrode voltage, which is required for control, can be obtained. Figure 1 shows the complete closed-loop system, including the optimal controller (solid line) and the simple controller using wall-shear stress feedback (dotted line). In the feedback loop using wall-shear stress feedback, the gain K is scalar.
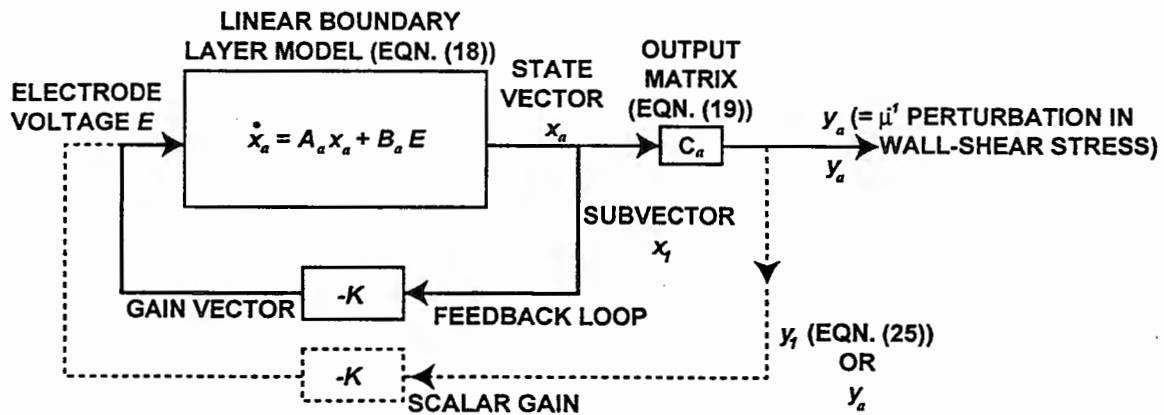
Figure 1. *Closed-Loop Lorentz Force Control System*

5. SIMULATION RESULTS

In this section the results of simulation using MATLAB® and Simulink™ software are presented. To derive the model, it is assumed that the normalized velocity is $U(y) = \sin(\pi(y+1)/4)$. The parameters chosen for high Reynolds number flow are $U_\infty = 17$(m/s), $h = (6.77/2)$mm; kinematic viscosity of water, $v = 11.4E\text{-}7\text{m}^2/\text{s}$, $v = \rho\mu$, $\ell_1 = 2\pi$; and density of water, $\rho = 1000$(kg/m^3). For simulation, the values $k_1 = 45$(N/m^3) and $q_0 = (1000/1\cdot3)(\text{m}^{-1})$ are used. These parameters are obtained from reference 13. The fundamental wave number is $\alpha_0 = 1$. For a choice of $M = 2$ in the series expansion (equation (10)), a sixth-order state variable model for each wave number is obtained. The three elements of the basis taken from reference 8 are

$$L_0(y) = 3 - 4T_2(y) + T_4(y),$$
$$L_1(y) = 2y - 3T_3(y) + T_5(y),$$
$$L_2(y) = 1.5T_3(y) - 2.5T_5(y) + T_7(y),$$

where $T_n(y)$ is the Chebyshev polynomial.[22]

For the chosen parameters, the matrices A_n, B_n, and C_n are computed. It is found that, except for matrix A_1, all other matrices, A_n, are stable. In fact, A_1, which is associated to wave number α_0, has a pair of unstable eigenvalues and the remaining four eigenvalues of A_1 are stable. For any nonzero initial condition the solution of the uncontrolled system diverges. A twelfth-order, open-loop system including the dynamics for wave numbers α_0 and $2\alpha_0$ was simulated with the initial condition $a_1(0) = b_1(0) = 1000(5\cdot4, 4\cdot05, 2\cdot7)^T$, and $a_2(0) = b_2(0) = a_1(0)/0\cdot18$. The divergent and oscillatory responses are shown in figure 2. The plots are shown for the velocity perturbations $u_1(x^*,y^*,t)$, $v_1(x^*,y^*,t)$ at the point $(x^*, y^*) = (0.75\ell_1,-0.409)$, and also for $C_f(x^*,-1,t)$, where $C_f = (\mu/0.5U_\infty^2)(\partial u_1/\partial y)$ is evaluated at $(x = x^*, y^* = 0)$. Although a control system can be designed to modify the responses of a set of modes, for simplicity, stabilization of dynamics of only the unstable mode is considered in this report. The spatial distribution of the Lorentz forces is assumed as given in equation (21) for the purpose of control.

Simulation results are obtained using an optimal control system and a simple controller that uses wall-shear stress feedback at one point. For simulation of the optimal controller, it is assumed that complete information on the state variable, x_1, of the subsystem associated with wave number α_0 to be controlled, is available. Unlike the optimal controller, synthesis of the simple controller is relatively easy, because only a measured signal at the wall is required for feedback. For optimal controller synthesis, each component of vector x_1 must be known.
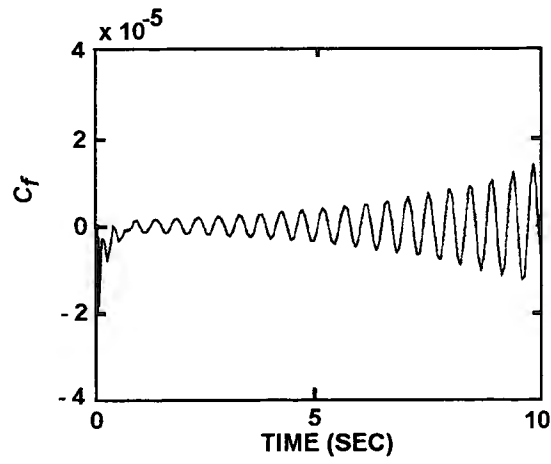
5.1 OPTIMAL CONTROL

Using the optimal control technique, a feedback controller was designed for the decoupled system in equation (22) describing the dynamics associated with the fundamental wave number. A quadratic term Qy_1^2 was used in the performance index with $Q = 0.01$ and $\lambda = 30$. The weighting matrix Q and λ were chosen after several trials by observing the simulated responses. The complete closed-loop system including the dynamics associated with wave numbers α_0 and $2\alpha_0$

and the feedback control law, $E = -Kx_1$, was simulated. The initial condition of figure 2 was retained. It was assumed that longitudinal control, $F_{111} = 1$; surface-normal control, $F_{121} = 1$; and the remaining parameters F_{1ik} in equation (21) were set to zero. Selected responses are shown in figures 3 and 4 using longitudinal and surface-normal force control, respectively. The plots are shown for the electrode voltage E, velocity perturbations $u_1(x^*,y^*,t)$, $v_1(x^*,y^*,t)$, and $C_f(x^*,0,t)$. In the closed-loop system, well-damped responses with moderate input voltage are observed. The corresponding interaction parameter $N^* = h$(Lorentz force/inertial force) is $0.0678E$, where the Lorentz force at the wall is $45E(N)$ and the inertial force is $(1/2)\mu(\partial U/\partial y)$ evaluated at the wall. As predicted, the surface-normal force control requires considerably larger electrode voltage compared to the longitudinal force control, since $\alpha_0 < -q$. It is important to note that using this control law, stabilization of all modes is accomplished, even if B_n, $n \neq 1$ are nonzero, since only exponentially decaying signal x_1 of the closed-loop system is superimposed on the stable dynamics for the remaining wave numbers. However, estimation of signal x_1 from measured signals must be made for the synthesis of the optimal controller.

5.2 STABILIZATION BY WALL-SHEAR STRESS FEEDBACK

Because the wall-shear stress is a constant multiple of du_1/dy, a simple feedback of the derivative of $du_1(x^*,y = 0,t)/dy$ is considered by choosing $E = -Kdu_1/dy$. In the derivative du_1/dy, the contribution of only the fundamental component x_1 of the state vector is retained and the higher harmonics are neglected. The gain K is chosen such that, in the closed-loop system, $(A_1 - KB_1C_1)$ is Hurwitz. Suitable values for longitudinal force control are $F_{112} = 1$ and $K = 0.05(U_\infty/h)$; and suitable values for surface-normal force control are $F_{121} = 0$ and $K = 0.05(U_\infty/h)q$. The feedback gains were selected after several trials so that the peaks in the electrode voltage are not too large during the transient period. The feedback gain K for stabilization is a function of the position x^* where the wall-shear stress is measured. With this choice of gains, the input influence matrix B_1 is the same for both force controls. The remaining parameters F_{1ik} were assumed to be zero. To reduce voltage magnitude, the initial conditions were chosen to be one-ninth the values of $(a_i(0), b_i(0))$ $(i = 1,2)$ assumed in section 5.1. Selected responses for the longitudinal and surface-normal force control are shown in figures 5 and 6.

The responses for u_1, v_1, and C_f are identical for the longitudinal and surface-normal force control. Unlike the optimal controller, responses are poorly damped and, in spite of smaller perturbations in the initial condition, considerably large electrode voltage is required. This result should not be a surprise because the optimal controller design requires complete information on x_1. For this simple control, (du_1/dy) feedback, which is merely a linear combination of state variables, is used. Larger peaks in the input voltage are observed for lateral control in this case also. For the choice of spatial distribution of Lorentz forces made, stability in the closed-loop system is preserved, even if the complete measured wall-shear stress including higher harmonics is fed back because the dynamics associated to all wave numbers except the fundamental one, are stable and the control input influence matrix $B_n = 0$ for $n = 0$ and $n > 1$. These responses can be improved when a feedback controller that uses wall-shear stress signals measured at several locations on the wall is designed.

14
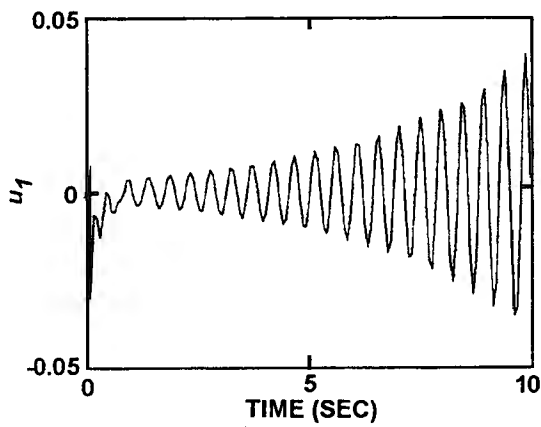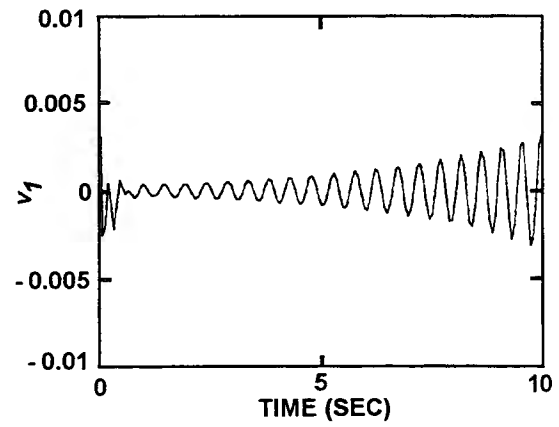
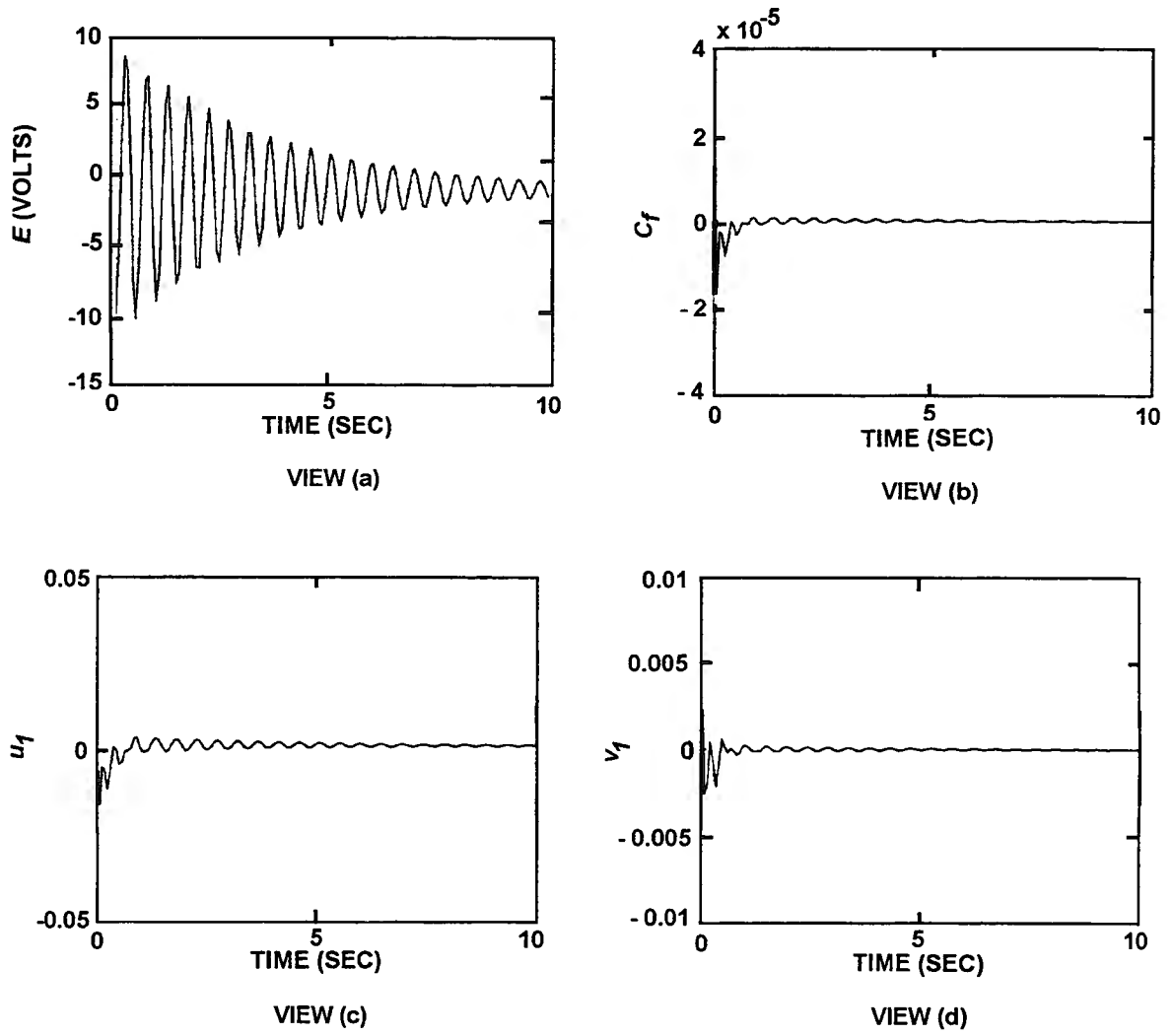*Figure 2. Uncontrolled System at* $x^* = 0.75\ell_1$, $y^* = -0.409$ *Above the Plate*

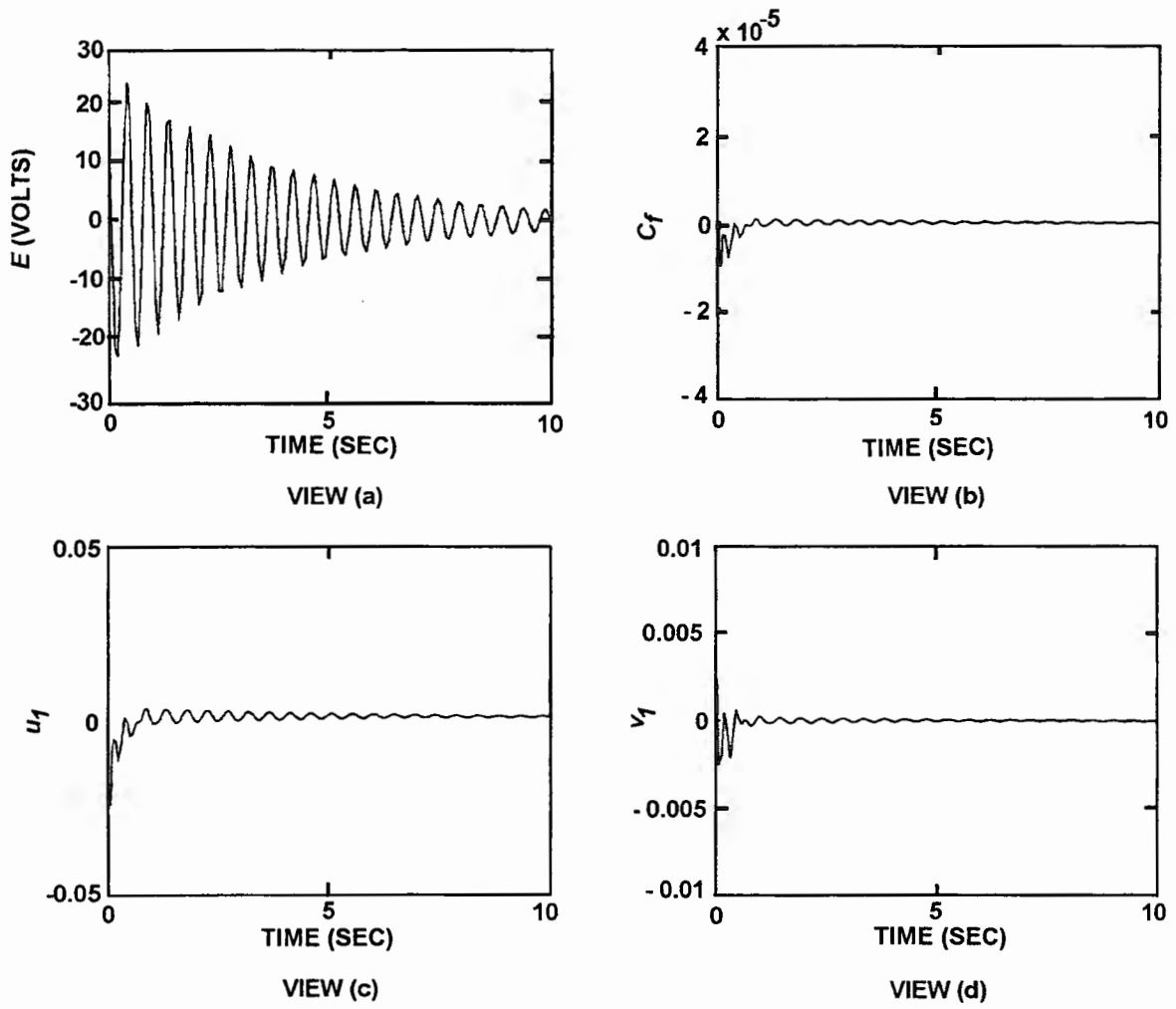*Figure 3. Optimal Longitudinal Force Control*
$(x^* = 0.75t_1 , y^* = -0.409)$

Figure 4. Optimal Surface-Normal Force Control
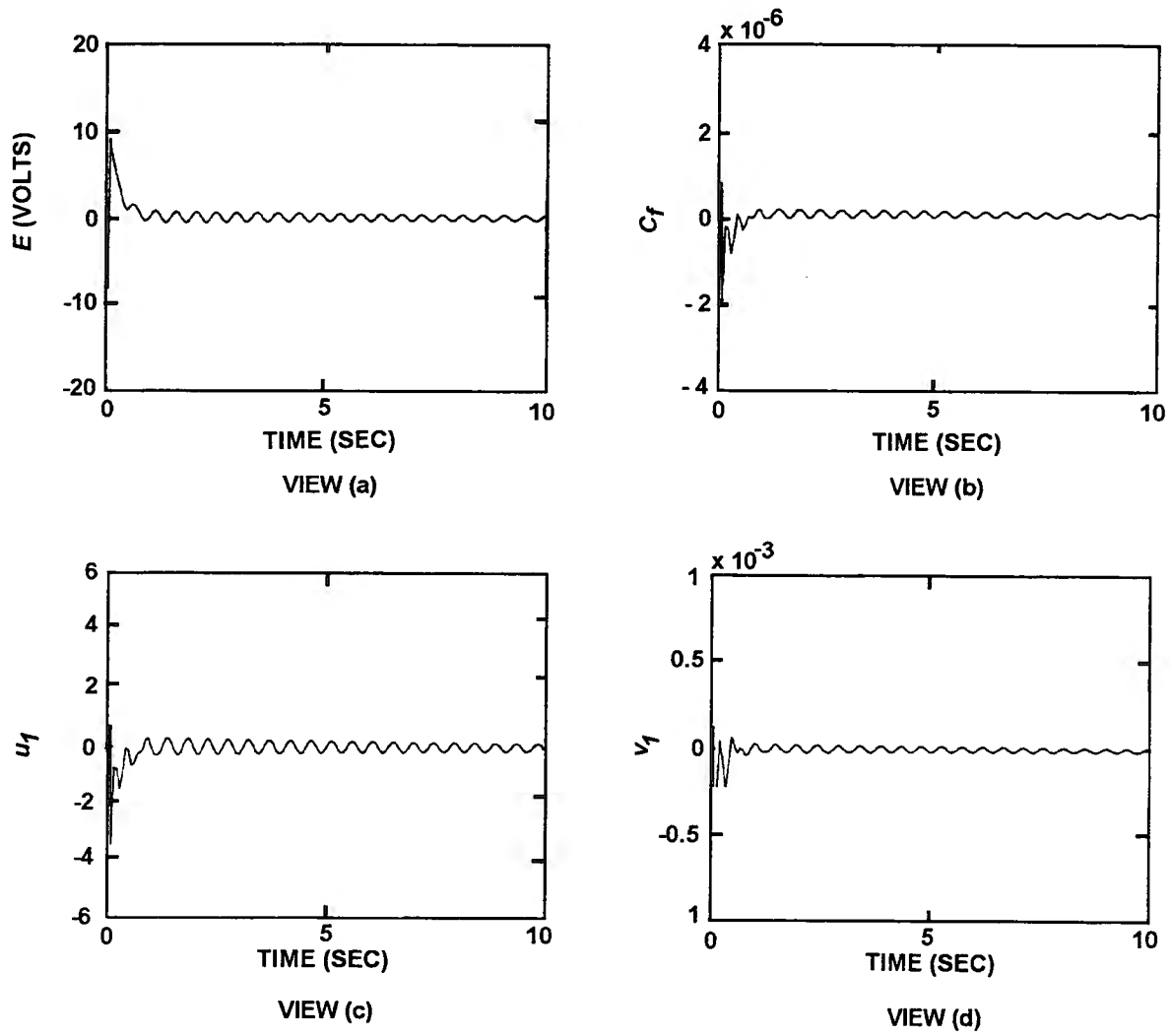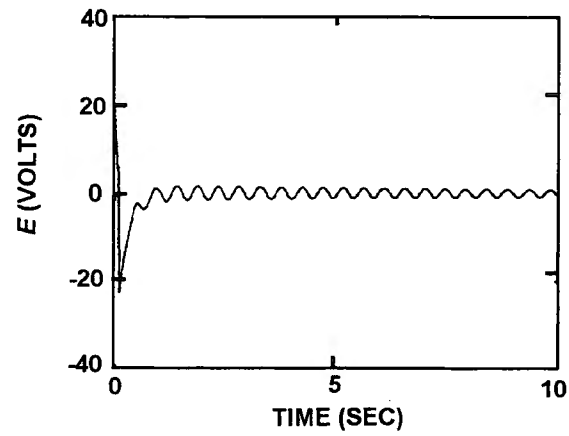$(x^* = 0.75t_1 , y^* = -0.409)$

Figure 5. Longitudinal Force Control by Wall-Shear Stress Feedback
$(x^* = 0.75\ell_1 , \ y^* = -0.409)$

NOTE: VARIABLES C_f, u_1, AND v_1 REMAIN UNDAMPED
AS IN FIGURE 5.

Figure 6. Surface-Normal Force Control by Wall-Shear Stress Feedback
(x* = 0.75t₁ , y* = -0.409)

6. CONCLUSIONS

This report examined a system-theory approach to the control of high Reynolds number sea water flow over a flat surface using electromagnetic forces produced by microtiles. Navier-Stokes equations, which include the effect of Lorentz forces, were linearized; and, using the Galerkin procedure, a linear, state variable model of finite dimension was derived. Based on this model, linear feedback control laws for system stabilization were obtained. It was shown that by judiciously selecting spatially distributed Lorentz forces, asymptotic stability in the closed-loop system can be accomplished using longitudinal and surface-normal force control. For lower wave numbers, longitudinal force control is more effective since it requires smaller electrode voltage to suppress velocity perturbations. However, a control system that uses wall surface normal force requires smaller electrode voltage compared with the longitudinal force controller when control of modes associated with higher wave numbers is desired. Although stabilization is possible using simple feedback of measured wall-shear stress signal, an optimal controller gives faster and well-damped responses. *However, for the synthesis of the optimal controller, it is necessary to design a state estimator to reconstruct the state for feedback using signals measured by the sensors.*

Several problems remain to be solved in this area: questions related to the effect of mode truncation, state estimation, control and observation spillover, digital implementation, and extension of the system-theory approach to nonlinearly perturbed dynamics, which plays a key role in turbulent flow, are all important and require further investigation.

7. REFERENCES

1. C. Crawford and G. Karniadakis, 1996, "Shear Stress Modification and Vorticity Dynamics in Near-Wall Turbulence," *Journal of Fluid Mechanics*, due to appear.

2. D. M. Bushnell, "Turbulent Drag Reduction for External Flows," AIAA Paper No. 83-0227, 1983.

3. P. R. Bandyopadhyay, "Review-Mean Flow in Turbulent Boundary Layers Disturbed to Alter Skin Friction," *Transcripts of the American Society of Mechanical Engineers (ASME) Journal Fluid Engineering*, vol. 108, 1986, pp. 127-140.

4. M. Gad-el-Hak, "Flow Control," *ASME Applied Mechanics Review*, vol. 9,1989, pp. 447-468.

5. H. W. Liepmann and D. M. Nosenchuck, "Control of Laminar Instability Waves Using a New Technique," *Journal of Fluid Mechanics*, vol. 118, 1982, pp. 187-200.

6. C. C. Lin, "Some Mathematical Problems in the Theory of the Stability of Parallel Flows," *Journal of Fluid Mechanics*, vol. 10, 1961, pp. 430-438.

7. R. W. Metcalfe, C. J. Rutland, J. H. Duncan, and J. J. Riley, "Numerical Simulation of Active Stabilization of Laminar Boundary Layers," *AIAA Journal*, vol. 9, 1986, pp. 1494-1501.

8. S. S. Joshi, "A Systems Approach to the Control of Transitional Flows," Ph.D Dissertation, University of California, Los Angeles, CA, 1996.

9. S. S. Joshi, J. L. Speyer, and J. Kim, "Modelling and Control of Two-Dimensional Poiseuille Flow," *Proceedings of the Conference on Decision and Control*, New-Orleans, LA., pp. 921-927, 1995.

10. C. Henoch and J. Stace, "Experimental Investigation of a Salt Water Turbulent Boundary Layer Modified by an Applied Streamwise Magnetohydrodynamic Body Force," *Physics of Fluids*, vol. 7, June 1995, pp. 1371-1383.

11. Private communication with D. Nosenchuck and G. Brown, Princeton University, Princeton, NJ, October 1991.

12. J. C. S. Meng, "Wall-Layer Microturbulence Phenomenology and a Markov Probability Model for Active Electromagnetic Control of Turbulent Boundary Layers in an Electrically Conducting Medium," NUWC-NPT Technical Report 10,434, Naval Undersea Warfare Center Division, Newport, RI, June 1995.

13. P. R. Bandyopadhyay, "Microfabricated Silicon Surfaces for Turbulence Diagnostic and Control," *Proceedings of the 1995 International Symposium on Active Control*, Newport Beach, CA, July 1995, pp. 1327-1338.

14. P. R. Bandyopadhyay and J. M. Castano, "Microtiles for Electromagnetic Turbulence Control in Salt Water—Preliminary Investigations," *Proceedings of the Fluids Engineering Division Conference*, San Diego, CA, November 1996.

15. F. F. Hatay, S. Biringen, and P. R. Bandyopadhyay, "Numerical Simulation of Flows Perturbed by Applied Lorentz Forces," *Bulletin of the American Physics Society*, vol. 40, no. 9, 1995, p. 2035.

16. Private communication among F. F. Hatay, S. Biringen, and P. R. Bandyopadhyay, 1996.

17. A. E. Perry and M. S. Chong, "On the Mechanism of Wall Turbulence," *Journal of Fluid Mechanics*, vol. 119, 1982, pp. 173-217.

18. P. R. Bandyopadhyay and R. Balasubramanian, "Vortex Reynolds Number in Turbulent Boundary Layers," *Theoretical and Computational Fluid Dynamics*, vol. 7, February 1995, pp. 101-118.

19. P. R. Bandyopadhyay and R. Balasubramanian, "Structural Modeling of the Wall Effects of Lorentz Force," *American Society of Mechanical Engineers. Transactions, Journal of Fluids Engineering*, vol. 118, June 1996, pp. 412-414.

20. S. A. Orszag, "Galerkin Approximations to Flows Within Slabs , Spheres, and Cylinders," *Physics Review Letters*, vol., 26, 1971, pp. 1100-1103.

21. C. A. J. Fletcher, *Computational Galerkin Methods*, Springer-Verlag, NY, 1984.

22. L. Fox and I. B. Parker, *Chebyshev Polynomials in Numerical Analysis*, Oxford University Press, London, 1968.

23. H. Schlichting, *Boundary-Layer Theory*, McGraw-Hill, NY, 1979.

24. T. Kailath, *Linear Systems*, Prentice-Hall, Englewood Cliffs, NJ, 1980.

INITIAL DISTRIBUTION LIST

Addressee	No. of Copies
Defense Technical Information Center (DTIC)	12
Defense Advanced Research Projects Agency (DARPA) (G. Jones)	1
Office of Naval Research (ONR-333; J. Fein, S. Lekoudis, L. Purtell, and E. Rood) (ONR-334; K. Ng) (ONR-342; T. McMullen)	6
NASA—Langley Research Center	1
University of Colorado at Boulder (S. Biringen)	1
University of California at Los Angeles (J. Kim)	1
University of Nevada at Las Vegas (S. Singh)	20
Applied Research Laboratory—Pennsylvania State University	1